Journal of Biomolecular NMR, **12:** 145–159, 1998.
KLUWER/ESCOM

NMR detection of slow conformational dynamics in an endonuclease toxin

Sara B.-M. Whittaker[a], Ruth Boetzel[a], Colin MacDonald[a], Lu-Yun Lian[b], Ansgar J. Pommer[c], Ann Reilly[c], Richard James[c], Colin Kleanthous[c] and Geoffrey R. Moore[a,*]
[a]*School of Chemical Sciences, University of East Anglia, Norwich NR4 7TJ, U.K.* [b]*Biological NMR Centre, P.O. Box 138, Maurice Shock Building, Leicester University, Leicester LE1 8HN, U.K.* [c]*School of Biological Sciences, University of East Anglia, Norwich NR4 7TJ, U.K.*

Received 22 December 1997; Accepted 23 February 1998

Key words: colicin, conformational dynamics, E9 DNase, EXSY

Abstract

The cytotoxic activity of the secreted bacterial toxin colicin E9 is due to a non-specific DNase housed in the C-terminus of the protein. Double-resonance and triple-resonance NMR studies of the 134-amino acid ^{15}N- and ^{13}C/^{15}N-labelled DNase domain are presented. Extensive conformational heterogeneity was evident from the presence of far more resonances than expected based on the amino acid sequence of the DNase, and from the appearance of chemical exchange cross-peaks in TOCSY and NOESY spectra. EXSY spectra were recorded to confirm that slow chemical exchange was occurring. Unambiguous sequence-specific resonance assignments are presented for one region of the protein, Pro^{65}-Asn^{72}, which exists in two slowly exchanging conformers based on the identification of chemical exchange cross-peaks in 3D ^{1}H-^{1}H-^{15}N EXSY-HSQC, NOESY-HSQC and TOCSY-HSQC spectra, together with C$^{\alpha}$ and C$^{\beta}$ chemical shifts measured in triple-resonance spectra and sequential NH NOEs. The rates of conformational exchange for backbone amide resonances in this stretch of amino acids, and for the indole NH of either Trp^{22} or Trp^{58}, were determined from the intensity variation of the appropriate diagonal and chemical exchange cross-peaks recorded in 3D ^{1}H-^{1}H-^{15}N NOESY-HSQC spectra. The data fitted a model in which this region of the DNase has two conformers, N_A and N_B, which interchange at 15 °C with a forward rate constant of 1.61 ± 0.5 s^{-1} and a backward rate constant of 1.05 ± 0.5 s^{-1}. Demonstration of this conformational equilibrium has led to a reappraisal of a previously proposed kinetic scheme describing the interaction of E9 DNase with immunity proteins [Wallis et al. (1995) Biochemistry, 34, 13743–13750 and 13751–13759]. The revised scheme is consistent with the specific inhibitor protein for the E9 DNase, Im9, associating with both the N_A and N_B conformers of the DNase and with binding only to the N_B conformer detected because the rate of dissociation of the complex of Im9 and the N_A conformer, N_AI, is extremely rapid. In this model stoichiometric amounts of Im9 convert, the E9 DNase is converted wholly into the N_BI form. The possibility that cis–trans isomerisation of peptide bonds preceding proline residues is the cause of the conformational heterogeneity is discussed. E9 DNase contains 10 prolines, with two bracketing the stretch of amino acids that have allowed the $N_A \rightleftharpoons N_B$ interconversion to be identified, Pro^{65} and Pro^{73}. The model assumes that one or both of these can exist in either the cis or trans form with strong Im9 binding possible to only one form.

* To whom correspondence should be addressed.

Abbreviations: 2D, two dimensional; 3D, three dimensional; Col, colicin; ColE9, colicin E9; CSI, chemical shift index; E9 DNase, the expressed C-terminal 134 amino acids of colicin E9 encompassing the DNase activity; EXSY, chemical exchange spectroscopy; HMQC, heteronuclear multiple quantum coherence; HSQC, heteronuclear single quantum coherence; NOE, nuclear Overhauser effect; NOESY, nuclear Overhauser effect spectroscopy; ppm, parts per million; TOCSY, total correlation spectroscopy; TPPI, time-proportional phase incrementation.

Introduction

Dynamic behaviour has long been regarded as being central to the properties of many proteins but its characterisation is not always easy (Creighton (1993) and references therein). Different kinds of motion occurring in different time regimes require a range of methods for their various rate constants and structural parameters to be obtained. NMR spectroscopy is a method capable of covering a range of time regimes – from rapid motions best characterised by relaxation time studies (Palmer (1997) and references therein) to extremely slow motions that can be detected by the appearance of slow chemical exchange behaviour. Sometimes slow chemical exchange can manifest itself by causing chemical exchange cross-peaks to appear in multidimensional NMR spectra recorded to enable scalar or dipolar connectivities to be determined (Jeener et al., 1979; Ernst et al., 1987) and there have been various reports of this phenomenon in recent years (e.g. Falzone et al. (1994) and Cai et al. (1997)). We have encountered this behaviour in our study of the DNase domain isolated from colicin E9, and report our observations in the present paper.

Colicin E9 (ColE9) is a plasmid-encoded DNase that is secreted as part of the stress response system of *Escherichia coli* (Luria and Suit, 1987; Eaton and James, 1989; James et al., 1996). The N-terminal 45 kDa region is responsible for binding ColE9 to the vitamin B_{12} receptor on target cells, which is encoded by the *btuB* gene (Di Masi et al., 1973), and translocating the cytotoxic C-terminal domain into the cell (Ohno-Iwashita and Imahori, 1980). The DNase activity is located in the 134-amino acid C-terminal domain (Wallis et al., 1994). To provide immunity against the action of the cytotoxic domain of ColE9, producing cells co-express a 9.5 kDa inhibitor protein, Im9 (Wallis et al., 1992a; James et al., 1996). This binds to both the intact ColE9 and the separate E9 DNase domain with a K_d of $\sim$0.1 fM in a binding process that involves a conformational change (Wallis et al., 1995b). Additional colicin DNases have been isolated (E2, E7 and E8), all with their own specific inhibitor proteins (Im2, Im7 and Im8, respectively) (Schaller and Nomura, 1976; Toba et al., 1988; Chak et al., 1991). There is a high degree of sequence similarity between the four colicin DNase domains ($\sim$80%), and between their inhibitor proteins ($\sim$50%), but only the cognate inhibitor provides complete immunity against the colicin E9 DNase action (James et al., 1992; Wallis et al., 1995b). However, non-cognate complexes are formed between the E9 DNase domain and Im2, Im7 and Im8 with K_d's ranging from 10^{-4} to 10^{-8} M (Wallis et al., 1995a).

We are engaged in a detailed kinetic, protein engineering and structural study of this system that has led to: the overexpression of the 134-amino acid DNase domain of ColE9 (Wallis et al., 1994) and the 86-amino acid Im9 (Wallis et al., 1992a); structural information from NMR studies concerning both free and bound Im9 (Osborne et al., 1994, 1996, 1997), including its 3D structure in solution; the identification of candidate specificity determinants for colicin DNases interacting with their immunity proteins (Curtis and James, 1991); the definition of the binding epitope on Im9 for the colicin E9 DNase by alanine-scanning and homologue-scanning mutagenesis (Li et al., 1997; Wallis et al., 1998); and the identification of putative active-site residues of the E9 DNase by random mutagenesis (Garinot-Schneider et al., 1996). In the present paper we report multinuclear NMR studies of unlabelled and $^{13}C/^{15}N$-labelled E9 DNase which have revealed that the E9 DNase has an unexpected dynamic structural heterogeneity that has led to a reappraisal of the kinetic mechanism previously proposed by us to describe the complexation of the E9 DNase with inhibitor proteins (Wallis et al., 1995a,b).

Experimental procedures

E9 DNase and Im9 were expressed in *Escherichia coli* and purified as previously described (Wallis et al., 1992b,1994). All samples prepared for NMR were assayed for biological activity as described by Wallis et al. (1992b,1994) and found to be fully active. Uniformly ^{15}N-labelled E9 DNase was obtained by growing the *E. coli* JM105 cells containing the expression system in minimal medium with $^{15}NH_4Cl$ (1g/l), and uniformly $^{13}C/^{15}N$-labelled E9 DNase was obtained from cells grown in minimal medium containing a mixture of $^{13}C_6$-glucose (4g/l) and $^{15}NH_4Cl$ (1g/l). Yields of protein from these enrichments were typically 20 mg/l.

NMR spectra were acquired with Bruker DMX500 and Varian Unity Inova 600 spectrometers. Spectra measured with the Bruker instrument were recorded by the States method (States et al., 1982); for gradient-enhanced experiments, sensitivity enhancements were also used (Kay et al., 1992). On the Varian instrument, quadrature detection was achieved in the indirectly acquired dimensions by the States-TPPI procedure (Mar-

ion et al., 1989b). Proton chemical shifts were measured from internal dioxane at 3.77 ppm and carbon chemical shifts were indirectly referenced to external sodium 3-(trimethylsilyl)propionate. ^{15}N chemical shifts were indirectly referenced to TSP by adjustment of the ^{1}H frequency of the methyl group of TSP to a corresponding ^{15}N frequency with the ^{1}H and ^{15}N gyromagnetic ratios.

The ^{1}H-^{1}H-^{15}N 3D TOCSY-HMQC and NOESY-HMQC pulse schemes (Zuiderweg and Fesik, 1989; Marion et al., 1989a) and the ^{1}H-^{1}H-^{15}N 3D TOCSY-HSQC and NOESY-HSQC pulse schemes (Zhang et al., 1994) were similar to those originally described. HNCO, HNCA, HN(CO)CA, CBCANH and CBCA(CO)NH spectra were recorded on the Bruker instrument as previously described (Grzesiek and Bax, 1992a,b,1993). Acquisition parameters are given in Table 1.

2D exchange spectra were acquired at 288 K with the Varian instrument using a clean-EXSY sequence to suppress cross-relaxation coherence transfer signals by Hartmann–Hahn mixing (Fejzo et al., 1991). The mixing scheme consisted of a delay τ_N to allow for longitudinal relaxation and a spin lock, $90^\circ_x - 90^\circ_{-x} - 90^\circ_{-x} - 90^\circ_x$, of duration τ_R to allow for transverse relaxation. Spectra with τ_N/τ_R ratios between 1:1 and 4:1, acquired with a mixing time of 100 ms, 256 increments and 128 transients, showed that a ratio of 3:1 gave better results for the E9 DNase in terms of signal:noise than the theoretical value of 2:1 expected for isotropic tumbling in solution. This suggests there is either an anisotropic contribution to the overall motion of the E9 DNase or its motional behaviour places it outside the spin diffusion limit. In order to resolve overlapping signals, the clean-EXSY sequence was incorporated into a standard ^{1}H-^{1}H-^{15}N 3D NOESY-HSQC experiment by replacing the mixing time with the EXSY mixing block described above. Spectra were acquired with a mixing time of 100 ms at 288 K.

Data were processed on Silicon Graphics Indigo work stations using FELIX (Biosym/MSI, California) or NMR-Pipe (Delaglio et al., 1995). A sine-bell squared window function was used for apodization in all dimensions with a phase shift of 60° in the acquisition dimension and 60°-70° in the indirect dimensions. Where necessary for the triple-resonance experiments, linear prediction was used to double the number of points in the heteronuclear dimensions.

Determination of rates of chemical exchange by NMR was carried out using the procedure of Jeener et al. (1979). Reversible exchange between two sites A and B may be represented as follows:

$$A \underset{k_{BA}}{\overset{k_{AB}}{\rightleftharpoons}} B$$

For pure chemical exchange (i.e. assuming no dipolar cross-relaxation during mixing), Jeener et al. (1979) showed that volumes of chemical exchange cross-peaks observed with the NOESY pulse sequence are related to the mixing time, τ_m by the following equation derived from the modified Bloch equations (Ernst et al., 1987):

$$\begin{aligned} I_{AB}(\tau_m) &= I_{BA}(\tau_m) \\ &= 0.5M \exp(-R_1\tau_m)[1- \\ &\quad \exp(-2D\tau_m)] \end{aligned} \quad (1)$$

where $I_{AB}(\tau_m)$ is the exchange cross-peak volume connecting sites A and B; $M = M_{A0}k_{BA} / 0.5(k_{AB}+ k_{BA}) = M_{B0}k_{AB} / 0.5(k_{AB} + k_{BA})$, where M_{A0} and M_{B0} denote the equilibrium magnetisation for species A and B, respectively, and k_{AB} and k_{BA} are exchange rate constants for the forward and backward reactions, respectively; R_1 is the spin-lattice relaxation rate, which is assumed to be equal for A and B; τ_m is the mixing time; and D is the average rate constant for the exchange process, defined as $0.5(k_{AB} + k_{BA})$.

At equilibrium,

$$x_A k_{AB} = x_B k_{BA} \quad (2)$$

where x_A, x_B are mole fractions of species A and B, respectively. For symmetrical two-site exchange ($x_A = x_B = 0.5$ and $k_{AB} = k_{BA}$), Eq. 1 simplifies to the more familiar Eq. 3:

$$\begin{aligned} I_{AB}(\tau_m) &= I_{BA}(\tau_m) \\ &= 0.5M_0 \exp(-R_1\tau_m)[1- \\ &\quad \exp(-2k\tau_m)] \end{aligned} \quad (3)$$

where M_0 is the total equilibrium magnetisation and k is the average rate constant for the exchange process. However, for systems where $x_A \neq x_B$, as in the case of the E9 DNase in which a major and minor conformer co-exist (see the Results section), this difference can be taken into account by substituting $k_{BA} = x_B k_{AB} / x_A$ into Eq. 1 to yield

Table 1. Acquisition parameters for NMR experiments on the E9 DNase

Experiment	B_0[a]	Data points				Sweep widths (Hz)				Offsets (ppm)[b]		References
		^1H	^{15}N	^{13}C	^1H	^1H	^{15}N	^{13}C	^1H	^{13}C	^{15}N	
CBCANH	500	512	36	60	–	7507.5	1666.7	8333.3	–	43.3	119.4	Grzesiek and Bax (1992a,b,1993)
CBCACONH	500	512	40	60	–	6775.0	1666.7	8333.3	–	43.3	119.4	Grzesiek and Bax (1992a,b,1993)
^1H-^1H-^{15}N EXSY--HSQC (τ_{mix} = 100 ms)	600	1024	16	–	128	8000	2500	–	8000	–	119.4	EXSY component based on Fejzo et al. (1991)
^1H-^1H-^{15}N NOESY--HSQC	600	1024	32	–	128	8000	1900	–	8000	–	119.4	Zhang et al. (1994)
(τ_{mix} = variable) for exchange rate				–	–			–	–	–	–	

[a]Experiments were run on Bruker DMX500 or Varian Unity Inova 600 spectrometers.
[b]The transmitter offset for the ^1H dimension was set to the frequency of the water resonance.

$$\begin{aligned} I_{AB}(\tau_m) &= I_{BA}(\tau_m) \\ &= x_A x_B M_0 \exp(-R_1\tau_m)[1- \\ &\quad \exp(-k_{AB}(1 + (x_B/x_A))\tau_m)] \end{aligned} \quad (4)$$

Equation 4 was used for the analysis of the E9 DNase dynamics presented herein.

Exchange rate constants were obtained from an analysis of a series of 3D ^{15}N-edited NOESY-HSQC spectra measured at 15 °C. 3D NOESY rather than EXSY spectra were used because the signal:noise in the latter is inferior. This is due to the fairly inefficient magnetisation transfer scheme required for selecting chemical exchange cross-peaks, which, as far as we are aware, is the only one to allow sufficient simultaneous suppression of both Hartmann–Hahn and cross-relaxation transfer effects. NOESY mixing times of 20, 30, 40, 50, 60, 70, 80, 100, 130, 160, 200 and 250 ms were employed to determine the build-up and decay of chemical exchange cross-peaks, and each experiment was acquired with 128 increments in t_1, 32 increments in t_2 and 8 scans per t_1 increment (Table 1). The total acquisition time for all 12 3D experiments was ~20 days. Volumes of exchange cross-peaks were measured manually in XEASY (Bartels et al., 1995) using the elliptical integration mode. Build-up curves obtained from plots of mixing time versus average exchange cross-peak volume/M_0 were fitted non-linearly according to Eq. 4 using the graphics software ORIGIN 4.1 (Microcal Software Inc.). Average exchange cross-peak volumes were plotted where cross-peaks were sufficiently resolved to allow integration since the individual cross-peak volumes for the forward and backward processes were not equal as would be expected at equilibrium, implying that the spin-lattice relaxation times are probably slightly different (±20 ms) for species A and B. Mole fractions x_A and x_B were obtained from the ratios of the diagonal peak volumes at $\tau_m = 0$ s of species A and B, respectively, over the sum of the diagonal peak volumes of A and B at $\tau_m = 0$ s. Diagonal peak volumes at $\tau_m = 0$ s were obtained from backward exponential extrapolation of the plot of mixing time versus diagonal peak volume. To ensure reproducibility, spectra at three mixing times (40, 60 and 80 ms) were measured on a separate occasion from the others in the series and the volumes of all the cross-peaks were normalised.

Results

Characterisation of E9 DNase

The ^1H-^{15}N HSQC spectrum (Figure 1) contains at least 240 NH cross-peaks (overlap prevents an exact count), many more than the 123 expected backbone amide peaks. Some of the additional resonances arise from side chains of the six asparagine, three glutamine and two tryptophan residues, and folded-back arginine resonances may also occur in this region. However, even if all of these are taken into account there are still too many cross-peaks for the reported amino acid sequence of the E9 DNase. A similar excess of resonances was observed in all triple-resonance NMR experiments correlating signals by scalar interactions; for example, the HNCO spectrum contains

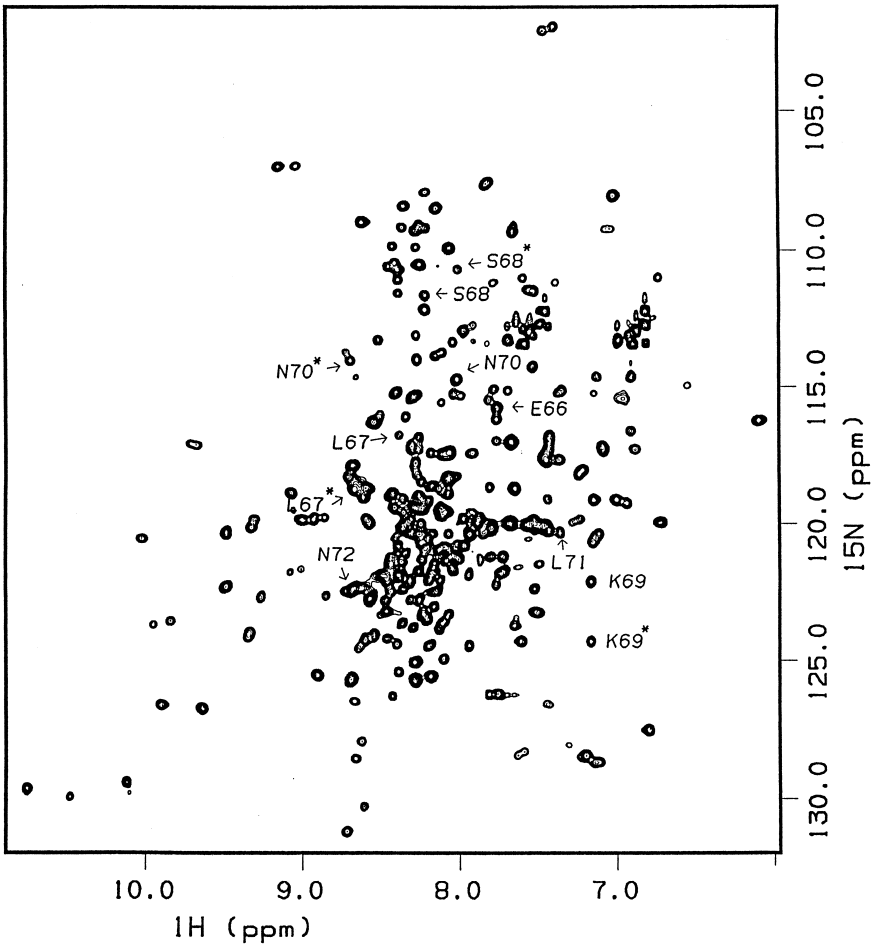

Figure 1. The 600 MHz ^{1}H-^{15}N HSQC spectrum of the ColE9 DNase in 90% H_2O/10% D_2O and 50 mM potassium phosphate buffer, pH 6.2, and at 293 K. Assignments for backbone amide peaks of Glu^{66}–Asn^{72} are indicated. ∗ denotes the minor conformation.

more than 185 peaks instead of the 123 backbone and 18 amide side-chain peaks, which are the maximum expected for the amino acid sequence (data not shown). The increase in the number of resonances over those expected suggests that there is some heterogeneity to the sample. Since electrospray mass spectra of E9 DNase samples consistently showed one species with the correct molecular mass (data not shown), any heterogeneity must result from variation in the conformations of individual molecules, and since molecular weight determinations made with an analytical ultracentrifuge have indicated that self-association does not occur, an intermolecular aggregation or dynamic association/dissociation process is ruled out as the cause of the heterogeneity (Pommer et al., 1998). Further NMR experiments indicate that at least some of the heterogeneity arises from dynamic processes as described below.

Chemical exchange cross-peaks and tryptophan indole resonances

There are three NH peaks in the tryptophan indole region of the ^{1}H-^{15}N HSQC spectrum of the E9 DNase with ^{1}H/^{15}N chemical shifts of 10.8/129.7 ppm, 10.5/129.9 ppm and 10.1/129.5 ppm (Figure 1). Connectivities between these NH resonances and tryptophan H2 and H7 resonances in NOESY and TOCSY spectra identify them as tryptophan indole resonances. However, there are only two tryptophans in the sequence, Trp^{22} and Trp^{58} (Eaton and James, 1989). This discrepancy can be accounted for by heterogeneity affecting at least one of the tryptophan indoles. Relatively intense cross-peaks between the resonances

at 10.8/129.7 ppm and 10.5/129.9 ppm in ^{1}H-^{1}H-^{15}N NOESY-HSQC and ^{1}H-^{1}H-^{15}N TOCSY-HSQC spectra (data not shown) are consistent with this explanation. Such a pattern of cross-peaks is not expected for any protein NH resonances in the absence of chemical exchange, other than those of arginine, asparagine or glutamine side chains, which can be eliminated as possible assignments by the connectivities to the tryptophan ring resonances and, for asparagine and glutamine, by the absence of corresponding HNCO peaks (data not shown). If slow chemical exchange between two sites for one of the indole NH groups is invoked, then the 10.8/129.7 ppm and 10.5/129.9 ppm cross-peaks can be attributed to chemical exchange cross-peaks, which do appear in TOCSY and NOESY spectra in some circumstances (Jeener et al., 1979; Ernst et al., 1987; Willem, 1987; Orrell et al., 1990; Falzone et al., 1994; Cai et al., 1997; Overmars and Altona, 1997).

To confirm that the 10.8/129.7 ppm and 10.5/129.9 ppm cross-peaks appearing in ^{1}H-^{1}H-^{15}N NOESY-HSQC and ^{1}H-^{1}H-^{15}N TOCSY-HSQC spectra are chemical exchange cross-peaks, a 2D ^{1}H-^{1}H EXSY spectrum was acquired which did indeed show there is a connectivity between the 10.8/129.7 ppm and 10.5/129.9 ppm peaks (data not shown).

Assignment of resonances

Sequence-specific resonance assignments have been obtained from 3D ^{1}H-^{13}C-^{15}N triple-resonance spectra. However, the structural heterogeneity inferred from Figure 1, and manifest in all 2D and 3D spectra, as Figure 2 shows for the Pro^{65}–Asn^{72} stretch, considerably complicates the assignment process, particularly the identification of sequential resonances based on analyses of both ^{1}H-^{13}C-^{15}N chemical shifts in 3D triple-resonance spectra and NOEs in ^{1}H-^{1}H-^{15}N NOESY-HSQC spectra. Thus, only incomplete assignment of spectra of the E9 DNase has so far been possible (S.B.-M. Whittaker and G.R. Moore, unpublished data). Nevertheless, it has been possible to unambiguously assign one region of the protein where the conformational heterogeneity is present: the region Pro^{65}–Asn^{72} (Figures 2 and 3 and Table 2). This was possible because, though the heterogeneity generally makes the assignment process difficult, in this case the identification of chemical exchange cross-peaks in 3D ^{1}H-^{1}H-^{15}N NOESY-HMQC/HSQC and TOCSY-HMQC/HSQC spectra, together with C$^{\alpha}$ and C$^{\beta}$ chemical shifts measured in triple-resonance spectra, aided assignments.

The identification of dipeptide units from triple-resonance NMR data led to the assignment of the unique Pro-Glu, Leu-Ser, Asn-Leu and Leu-Asn dipeptides (Figure 2). However, two distinct Leu-Ser dipeptide units were detected (Table 2). Also, at least six potential Ser-Lys dipeptides were observed, although the sequence only contains four such units: residues 3/4, 62/63, 68/69 and 80/81 (Eaton and James, 1989). However, the only C$^{\alpha}$ and C$^{\beta}$ chemical shift matches for the two Leu-Ser dipeptides, residues 67/68, are those shown in Table 2. A combination of the sequential NOEs and chemical exchange relationships observed in the 200 ms ^{1}H-^{1}H-^{15}N NOESY-HSQC spectrum (Figure 3), together with the C$^{\alpha}$ and C$^{\beta}$ chemical shifts obtained from triple-resonance spectra (Figure 2), has allowed resonances of the Pro^{65}–Asn^{72} region to be assigned (Table 2). This assignment scheme predicts that up to five NH-NH chemical exchange cross-peaks for this region should be observed in a 3D ^{1}H-^{1}H-^{15}N EXSY-HSQC. The appropriate slices of this reveal that the chemical exchange cross-peaks expected for Leu^{67}, Ser^{68} and Asn^{70} are indeed observed (Figure 4), as the NOESY-HSQC slices of Figure 2 indicate they should be. The difference in NH ^{1}H chemical shifts for Lys^{69} and Leu^{71} may be too small for chemical exchange cross-peaks to be detected in the 3D spectrum. Nevertheless, the observed 3D EXSY connectivities confirm the description given in Table 2.

Rate measurements

Conformational exchange rates have been determined for the amide hydrogens of residues Leu^{67}, Ser^{68} and Asn^{70}, and the side-chain NH of the tryptophan, all of which exhibit exchange cross-peaks in the 3D ^{15}N-edited NOESY-HSQC spectrum (Figure 3). Lys^{69} and Leu^{71} also exhibit heterogeneity (Figure 2), but since the amide hydrogen chemical shifts of the two forms are very similar for each residue (Table 2), the corresponding exchange rates could not be measured. 2D slices through the 3D NOESY spectrum showing the amide hydrogen of Ser^{68} in one of its conformations illustrate both the build-up and decay of diagonal and exchange cross-peak intensities with mixing time, and the degree of overlap between the diagonal and cross-peak for a relatively well-resolved signal (Figure 5). The mixing time dependencies of the diagonal and cross-peak volumes for Ser^{68} (Figure 6) show that the diagonal peak decays exponentially whilst the chemical exchange cross-peak has a rapid build-up phase and a competing decay arising from relaxation (Eq. 4).

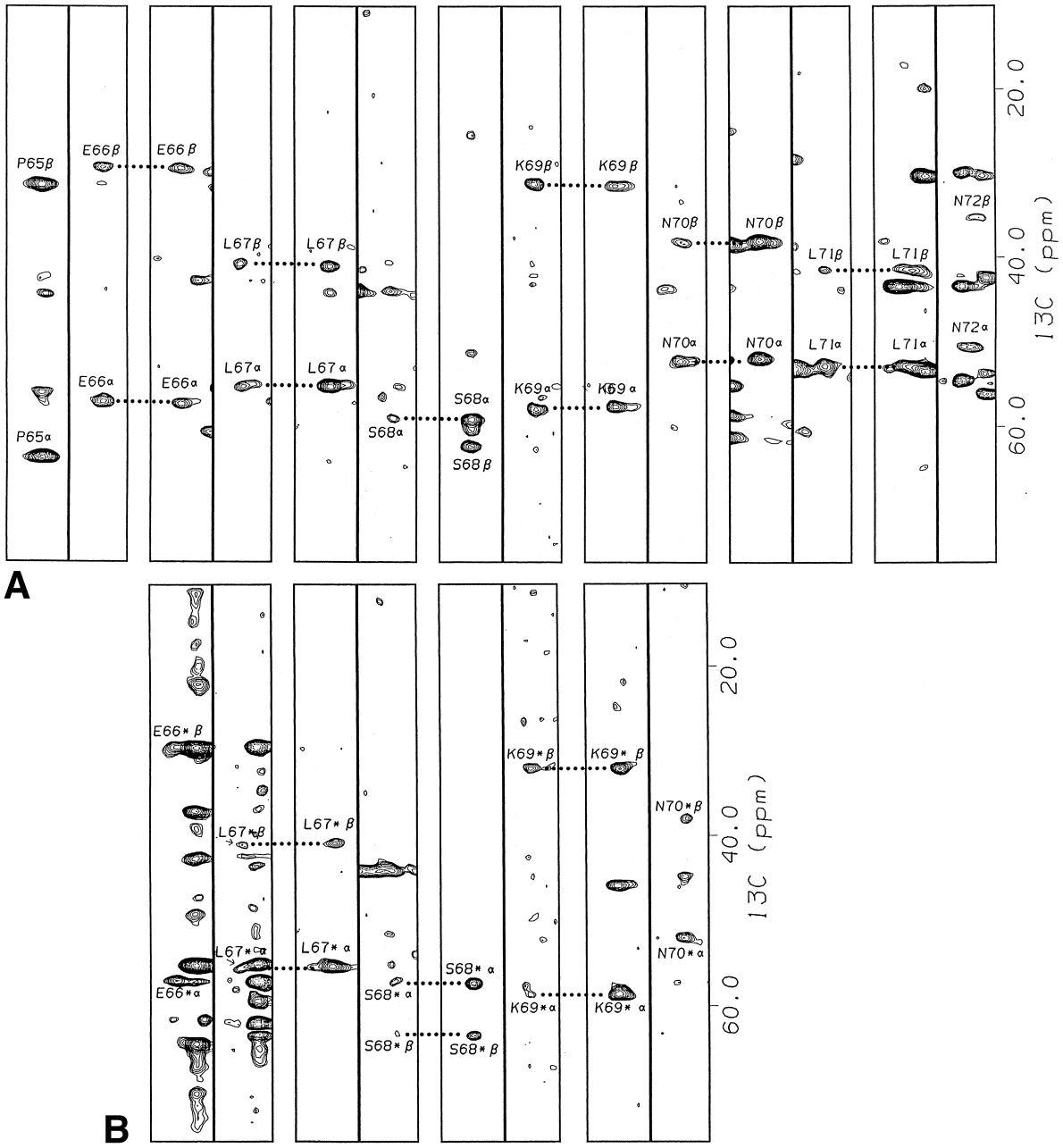

Figure 2. 2D slices taken along the ^{15}N dimension of 500 MHz. triple-resonance 3D spectra illustrating the assignment of sequential dipeptide units in the region Pro^{65}–Asn^{72} [P-E-L-S-K-N-L-N]. The upper series of spectra (A) come from the major N_B form of the DNase and the lower series (B) from the minor N_A form (see text). At each ^{15}N chemical shift, the left slice is from a CBCA(CO)NH spectrum and the right slice is from a CBCANH spectrum.

Table 2. Chemical shifts[a] of resonances of Pro^{65}–Asn^{72} [b]

Residue	Conformer N_B					Conformer N_A									
	N′	NH	C′	C^α	C^β	N′	NH	C′	C^α	C^β	ΔN′	ΔNH	ΔC′	ΔC^α	ΔC^β
Pro^{65}	n.d.[c]	∗[c]	178.10	63.71	31.40	n.d.	∗	n.d.	n.d.	n.d.	n.d.	∗	n.d.	n.d.	n.d.
Glu^{66}	115.96	7.82	178.46	57.12	29.30	n.d.	n.d.	178.79	57.20	29.60	n.d.	n.d.	0.33	0.08	0.30
Leu^{67}	116.87	8.42	179.33	55.27	40.77	118.76	8.70	179.51	55.36	40.85	1.89	0.28	0.18	0.09	0.08
Ser^{68}	111.73	8.27	176.48	58.86	62.36	110.81	8.07	175.49	57.39	63.49	−0.92	−0.20	−0.99	−1.47	1.13
Lys^{69}	122.05	7.22	177.05	58.04	31.35	123.93	7.21	177.14	58.82	32.13	1.88	−0.01	0.09	0.78	0.78
Asn^{70}	114.82	8.05	174.98	52.22	38.23	114.11	8.74	175.12	52.07	38.03	−0.71	0.69	0.14	−0.15	−0.20
Leu^{71}	120.23	7.52	176.22	53.03	41.45	120.07	7.39	n.d.	53.30	44.50	0.16	−0.13	n.d.	0.27	0.05
Asn^{72}	122.35	8.68	n.d.	50.76	35.29	n.d.	n.d.	n.d.	n.d.	n.d.	n.d.	n.d.	n.d.	n.d.	n.d.

[a]Chemical shift values were determined at 293 K with ∼2 mM samples of E9 DNase in 25 mM sodium phosphate, pH 6.2.
[b]The DNase exists in multiple conformations, two of which have been designated as N_A and N_B (see text). The chemical shifts of some of the backbone (N′, NH, C^α and C′) and side chain (C^β) resonances for these two conformers differ. The difference values ($N_A - N_B$) are designated with Δ.
[c]n.d.: not determined; ∗: resonance not present.

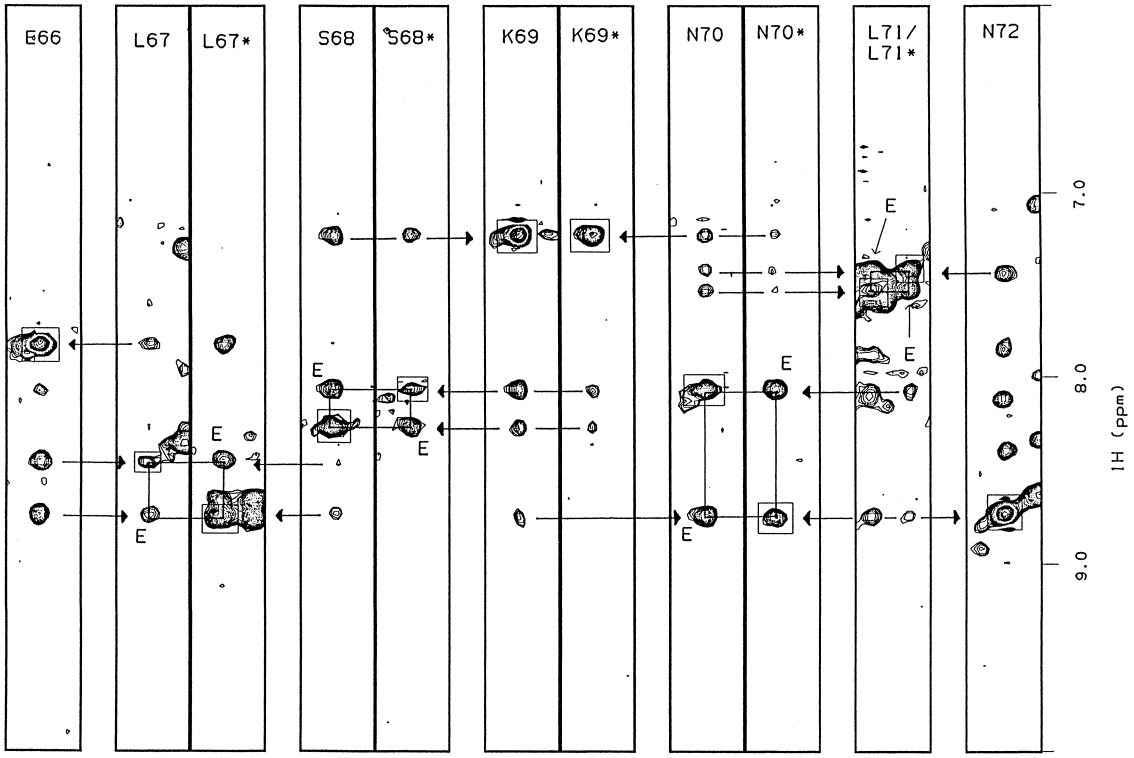

Figure 3. Slowly exchanging conformational heterogeneity of the Pro^{65}-Asn^{72} region [P-E-L-S-K-N-L-N] detected by the appearance of chemical exchange cross-peaks in the amide region of ^1H-^1H-^{15}N NOESY-HSQC spectra at 288 K. The most intense NH-NH cross-peaks, labelled E, are chemical exchange cross-peaks. The weaker NH-NH cross-peaks are NOE cross-peaks. Diagonal peaks are boxed. Horizontal arrows indicate sequential $d_{NN}(i,i+1)$ and $d_{NN}(i,i-1)$ connectivities. For Lys^{69} the chemical exchange cross-peaks overlap with the diagonal.

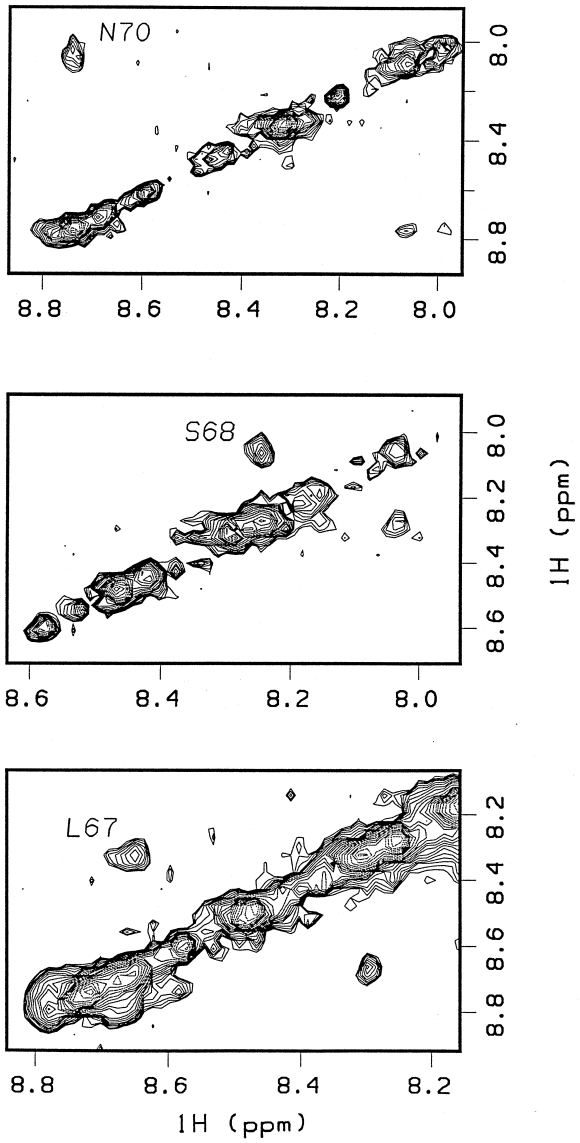

Figure 4. Slowly exchanging conformational heterogeneity of the Leu^{67}–Asn^{70} region detected in a ^{1}H-^{1}H-^{15}N EXSY-HSQC spectrum at 288 K. Each 2D slice is taken at the ^{15}N chemical shift of the NH for the given residue.

These data give an indication of the accuracy with which the diagonal peak volumes describe the equilibrium magnetisation, and hence mole fractions for species A and B. For the Leu^{67}, Ser^{68}, Asn^{70}, and tryptophan indole NH signals, the equilibrium constants for the exchange process determined from the ratio of the mole fractions are 1.64 ± 0.10, 2.05 ± 0.12, 1.15 ± 0.05 and 1.31 ± 0.09, respectively. Relatively good fits were obtained for the cross-peak volumes of all amide NH signals analysed (Figures 6 and 7) despite the difficulty encountered with accurate volume measurement resulting from severe peak overlap. Rate constants determined as the average of the forward and backward rates for the exchange process were found to be: 1.53 ± 0.10 s^{-1}, 1.46 ± 0.09 s^{-1}, 0.86 ± 0.08 s^{-1} and 1.47 ± 0.13 s^{-1}, for Leu^{67}, Ser^{68}, Asn^{70} and the tryptophan side-chain NH, respectively. Overlap was especially problematic for Leu^{67} and Ser^{68}. The amide hydrogen of Leu^{67} in one conformation overlaps with the amide hydrogen of Arg^{37} (8.68/118.9 ppm) while the amide hydrogen in the other conformation overlaps with an unassigned spin system that exhibits a NOESY cross-peak at the same chemical shift as the exchange cross-peak for this conformation. For both forms of Leu^{67}, the appropriate diagonal peak volumes, obtained from backward exponential extrapolation to $\tau_m = 0$ s, were halved to take account of the overlap. For exchange rate evaluation of Ser^{68}, rather than averaging the two cross-peak volumes corresponding to the forward and backward rate processes, the exchange cross-peak volume for only one of the rate processes was used, because accurate volume measurement was impossible for one conformation as its diagonal peak overlapped the corresponding exchange cross-peak. Nevertheless, the result obtained agrees well with the other rates determined. In the case of the tryptophan side-chain NH (Figure 7), a larger cross-peak volume error exists at longer mixing times, even though these cross-peaks are isolated in the spectrum, because the low intensity of the exchange cross-peaks prevents accurate volume integration.

The quoted errors reflect the uncertainty in the peak volume integrations but the problem of peak overlap is another potential source of error, though one not quantifiable for individual groups. The spread of values for different groups is a better estimate of error than the uncertainty in the peak volume integrations, as indicated by the average values of the rate and equilibrium constants: the average value of the forward and backward rate constants for Leu^{67}, Ser^{68}, Asn^{70} and the tryptophan side-chain NH is 1.33 ± 0.47 s^{-1} and the average value of the equilibrium constant is 1.54 ± 0.51, with the error bars determined from the ranges of the individual equilibrium and rate constants. The error bars to one standard deviation for the average values of the equilibrium constant and the average of the forward and backward rate constants originating from the volume integrations are 1.54 ± 0.40 and 1.33 ± 0.33 s^{-1}. Thus, the error bars determined from the spread of individual values are only marginally greater than those from the

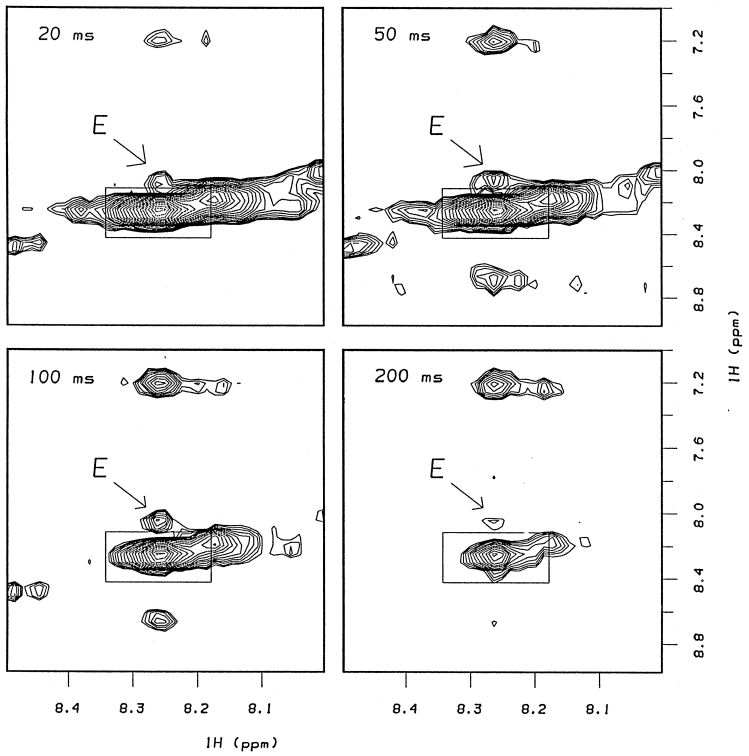

Figure 5. 2D slices through ^{1}H-^{1}H-^{15}N NOESY-HSQC spectra at 288 K recorded with different mixing times illustrating the variation of exchange cross-peak and diagonal intensities for the NH of Ser^{68} at 8.27/111.7 ppm. The diagonal peak is boxed; E indicates the chemical exchange cross-peak between the NH hydrogens in the two conformations.

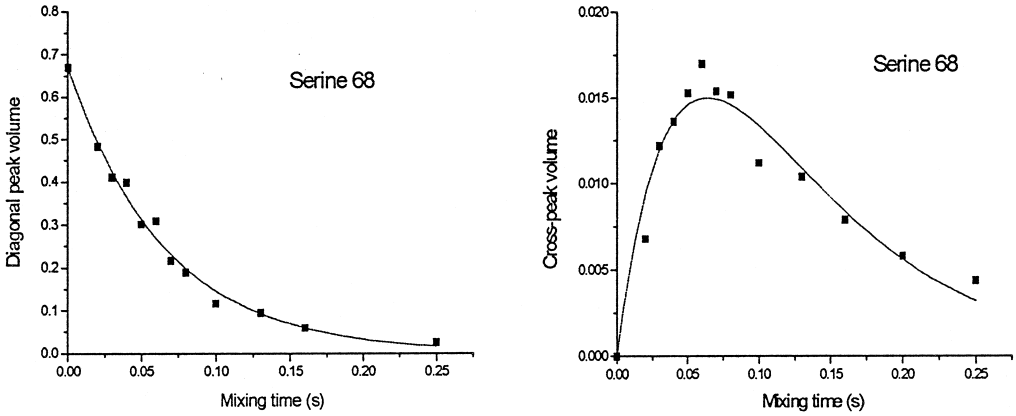

Figure 6. Build-up and decay curves for the chemical exchange cross-peak and diagonal peak of the NH of Ser^{68} at 8.27/111.7 ppm in ^{1}H-^{1}H-^{15}N NOESY-HSQC spectra at 288 K. Diagonal and cross-peak volumes plotted correspond to measured peak volumes divided by M_0 (see text). The decay curve for the diagonal peak indicates the mole fraction for this conformation to be 0.67 ± 0.04. The mixing time variation of cross-peak volumes was fitted to Eq. 4 to yield $(k_{AB} + k_{BA})/2 = 1.46 \pm 0.09\ s^{-1}$, and $R_1 = 14.3 \pm 0.7\ s^{-1}$.

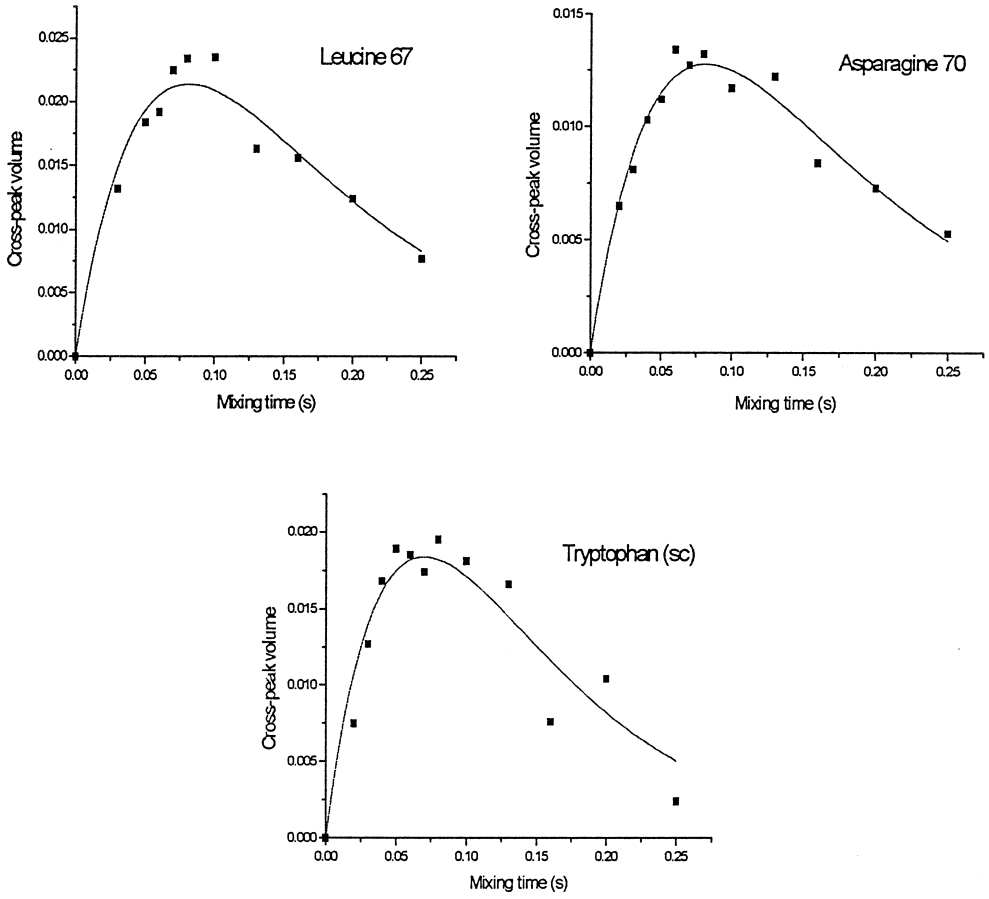

Figure 7. Build-up curves for chemical exchange cross-peaks in ^{1}H-^{1}H-^{15}N NOESY-HSQC spectra at 288 K. Cross-peak volumes correspond to the average volume of the two exchange cross-peaks observed for each NH divided by M_0 (see text). The following rates were obtained for Leu^{67}, Asn^{70} and the tryptophan side chain, respectively: $(k_{AB} + k_{BA})/2 = 1.53 \pm 0.10\ s^{-1}$, $0.86 \pm 0.08\ s^{-1}$ and $1.47 \pm 0.13\ s^{-1}$; and $R_1 = 10.9 \pm 0.5\ s^{-1}$, $11.4 \pm 0.4\ s^{-1}$ and $12.9 \pm 0.9\ s^{-1}$.

peak integrations. The average forward rate constant is $1.61 \pm 0.5\ s^{-1}$ and the average backward rate constant is $1.05 \pm 0.5\ s^{-1}$ calculated from the average rate constant, $1.33 \pm 0.47\ s^{-1}$, and the average equilibrium constant, 1.54 ± 0.51.

The agreement between the rate and equilibrium constants obtained from the analysis of the 3D NMR data is striking given the difficulties in determining peak volumes, and it is doubtful whether the differences in rate and equilibrium constants measured for different resonances are significant. However, it is not certain that the dynamic process affecting the groups investigated is the same in all cases. The indole NH of the tryptophan in particular, need not follow the same exchange pathway as the backbone nuclei since it may experience additional flexibility about its C^{α}-C^{β} bond. However, as we have no additional data to address this point we shall describe the conformational interchange detected in these experiments as if it is a single process.

Discussion and Conclusions

NMR spectroscopy of slowly interchanging protein conformations

Though of considerable mechanistic interest, the slow conformational dynamics observed for the E9 DNase has considerably complicated determination of its structure by NMR. Because of the presence of more peaks than expected from the amino acid sequence, resonances are extensively overlapped, and because there are multiple conformations, the concentrations of individual conformations are relatively low, leading

to poor signal:noise ratios in some spectra. Thus, spectra have not been completely assigned. Also there are relatively small numbers of long-range NOEs detected in 3D NOESY-HSQC spectra, perhaps reflecting the effect of conformational dynamics on the build-up and decay of NOEs (S.B.-M. Whittaker and G.R. Moore, unpublished data). Despite these problems however, it has been possible to unambiguously assign peaks from a region of the protein undergoing slow chemical exchange. Slices from a 3D ^{1}H-^{1}H-^{15}N EXSY-HSQC spectrum (Figure 4) were central to this analysis. However, 3D NOESY spectra rather than EXSY spectra were used to quantify the exchange rates because their signal:noise was better.

Chemical shift and structural heterogeneity

As described above, the presence of structural heterogeneity was inferred from the observation of too many cross-peaks in all of the multidimensional spectra and from the detection of chemical exchange cross-peaks. Many cross-peaks appeared to be doubled, an effect manifested in 3D spectra by peaks generally having common chemical shifts in one or two dimensions but slightly different chemical shifts in the other dimension(s). It is notable that within the Pro^{65}–Asn^{72} region there is a variation in chemical shift difference between the two conformers which, for the C$^{\alpha}$ and C$^{\beta}$ resonances, is at a maximum for Ser^{68} and Lys^{69}. These are in the middle of the region and thus the conformational dynamics might simply involve movement of this stretch of amino acids between two environments with Glu^{66} and Leu^{71} acting as hinges. However, it is clear from the chemical exchange effect with either Trp^{22} or Trp^{58}, and the much greater number of peaks in the ^{1}H-^{15}N HSQC spectrum than predicted from the sequence (Figure 1), that the conformational heterogeneity is far more extensive than that discussed for the Pro^{65}–Asn^{72} region.

Chemical shift heterogeneity indicating multiple forms of proteins in solution has been reported by many authors (e.g. Falzone et al. (1994), Overduin et al. (1996), Adjadj et al. (1997), Cai et al. (1997) and Carlomagno et al. (1997)). In most cases the origin of the heterogeneity has not been reported, though a relatively common cause is cis–trans isomerisation of peptide bonds preceding proline residues. This has been observed for various peptides (Thomas and Williams, 1972; Maia et al., 1976; Cheng and Bovey, 1977; Grathwohl and Wüthrich, 1981; Adjadj et al., 1997) and several proteins including staphylococcal nuclease (Evans et al., 1987; Hinck et al., 1990; Truckses et al., 1996), human interleukin-3 (Feng et al., 1995,1996), and calbindin D$_{9K}$ (Chazin et al., 1989; Kördel et al., 1990). Given the large number of proline residues in the E9 DNase, 10 out of 134 (Eaton and James, 1989), and the observation that the residues listed in Table 2 with relatively large chemical shift differences between the two conformers are located about midway between two prolines, Pro^{65} and Pro^{73}, the question is raised as to whether the dynamic heterogeneity exhibited by the E9 DNase is connected with proline cis-trans isomerisation. The rate constants for the DNase conformational dynamics are similar to those for proline cis-trans isomerism in peptides (Steinberg et al., 1960; Maia et al., 1976; Schmid and Baldwin, 1978), as are the activation enthalpies if the activation energy for the E9 DNase conformational equilibrium reported by Wallis et al. (1995b) is for the process described in this paper (see below).

Possible functional significance of the DNase conformational exchange

We have reported previously that on complex formation between Im9 (I) and the E9 DNase domain (N), there is a 15–20% enhancement of the tryptophan fluorescence emission emanating from the DNase that has a biphasic time dependence (Wallis et al., 1994,1995b). To account for these observations, we proposed the two-step binding profile shown in Scheme 1.

$$\mathrm{N} + \mathrm{I} \rightleftharpoons \mathrm{NI}^{*} \rightleftharpoons \mathrm{NI}$$

Scheme 1.

The rapid formation of a collision complex, NI*, was followed by its slow rearrangement to give the final product complex, NI. However, in our earlier work we noted that other kinetic schemes were consistent with the stopped-flow data presented, including that shown as Scheme 2 (Wallis et al., 1995b).

$$\mathrm{N_A} \rightleftharpoons \mathrm{N_B} \overset{+\mathrm{I}}{\underset{-\mathrm{I}}{\rightleftharpoons}} \mathrm{N_B I}$$

Scheme 2.

In this scheme the E9 DNase exists in two conformational states (N_A and N_B), only one of which (N_B) is able to bind Im9. Association of Im9 with N_B remains the rapid process detected by stopped-flow measurements, but it is the interconversion of the unbound nuclease rather than the nuclease–Im protein complex that is the slow step.

Table 3. Kinetic and thermodynamic parameters for assuming that N_AI is not present in appreciable amounts. Scheme 3

Parameter	Wallis et al. (1995b)[a]	This work[b]
k_1	n.d.	$1.61 \pm 0.5\ s^{-1}$
k_{-1}	n.d.	$1.05 \pm 0.5\ s^{-1}$
$k_1 + k_{-1}$	$4.4\ (\pm 0.4)\ s^{-1}$	$2.66 \pm 1.0\ s^{-1}$ [c]
	$[1.0\ (\pm 0.4)\ s^{-1}]$ [c]	
k_2	$9.0\ (\pm 0.5) \times 10^7\ M^{-1}\ s^{-1}$	n.d.
k_{-2}	$2.2\ (\pm 0.2) \times 10^{-6}\ s^{-1}$	n.d.
K_1	n.d.	1.54 ± 0.51
K_2	n.d.	$\sim 2.7 \times 10^{13}\ M^{-1}$ [d]
$K_d = (K_1K_2)^{-1}$	$2.4\ (\pm 0.4) \times 10^{-14}\ M$	n.d.
k_4	n.d.	$\sim 10^0 - 10^{-3} \times k_2$
k_{-4}	n.d.	$\gg k_{-2}$
K_3	n.d.	$\gg K_1$
K_4	n.d.	$\ll K_2$

[a] All parameters were determined for experiments conducted in 50 mM Mops buffer, pH 7.0, containing 200 mM NaCl at 298 K except for the value of $k_1 + k_{-1}$ in brackets which was determined at 288 K.

[b] NMR experiments were carried out with samples in 90% H_2O/10% D_2O and 50 mM potassium phosphate buffer, pH 6.2, at 288 K.

[c] Although the correspondence between the stopped-flow fluorescence and NMR determined rates for $k_1 + k_{-1}$ is not exact, the agreement is reasonable, especially if the exchange process is cis–trans isomerisation of peptide bonds preceding proline residues as the rates of these are known to increase with decreasing pH (Steinberg et al., 1960).

[d] Value of K_2 obtained from the K_d reported by Wallis et al. (1995b) and the K_1 determined in this work.

If the DNase conformational exchange described in the present paper is the same slow process detected in the stopped-flow kinetics, then we need to revise our proposal of the mechanism of DNase–Im association and dissociation. The fact that both the NMR experiments and the stopped-flow measurements determine approximately the same rate (Table 3) for a conformational change affecting one of the two tryptophans of the DNase supports the case for adopting Scheme 2 in favour of Scheme 1. Table 3 lists the kinetic and thermodynamic parameters associated with Scheme 2. The re-evaluation of the kinetic scheme describing the formation of the DNase-Im complex does not change the interpretation of the kinetic data obtained with mutant forms of Im9 that we have proposed maps out the DNase binding site on Im9 in terms of binding energies (Li et al., 1997; Wallis et al., 1998).

Adopting Scheme 2 raises a number of questions that can be explored with the full square thermodynamic cycle (Scheme 3) for which $K_n = k_n/k_{-n}$ and $K_1K_2 = K_3K_4$.

$$
\begin{array}{ccc}
 & \overset{k_1}{\rightleftharpoons} & \\
N_A & \underset{k_{-1}}{} & N_B \\
k_{-4} \Downarrow k_4 & & k_{-2} \Downarrow k_2 \\
-I \quad +I & & -I \quad +I \\
 & \overset{k_3}{\rightleftharpoons} & \\
N_AI & \underset{k_{-3}}{} & N_BI
\end{array}
$$

Scheme 3.

With $K_1 = K_3$ and $K_2 = K_4$, N_AI and N_BI would be present in solution in the same ratio as N_A and N_B. This is unlikely for two reasons. First, with $K_2 = K_4$, $k_2 = k_4$, $k_2 = k_1$, and with $K_1 \cong 1.5$, the conformational equilibrium of the DNase would not produce biphasic stopped-flow fluorescence traces, as observed by Wallis et al. (1995b). Second, if the Im9 binding site on N_A and N_B differed, it is likely that the NMR spectra of the Im9 bound to the two sites would also be different, but ^1H-^{15}N NMR studies of ^{15}N-labelled Im9 binding to unlabelled E9 DNase have shown only one form of bound Im9 (Osborne et al., 1997). Thus, we conclude that $K_1 \neq K_3$ and $K_2 \neq K_4$. We can go further than this: for example, if N_AI is not present in solution in appreciable amounts then $K_3 \gg K_4$, $K_3 \gg K_1$ and $K_2 \gg K_4$.

The rate of association of Im9 with N_B (k_2) has been found to be $9 \times 10^7\ M^{-1}s^{-1}$ at pH7 (50 mM Mops, 200 mM NaCl) (Wallis et al., 1995b). At lower ionic strength the rate is almost 10^3 times faster, indicating that long-range electrostatic interactions between the approaching molecules might speed up the rate of the association. Even if N_A had an appreciably different conformation from N_B, k_4 should be substantial as the differences between N_A and N_B would not prevent N_A from colliding with Im9. Thus, to get a low K_4 to allow $K_2 \gg K_4$, the rate of dissociation of the N_AI form of the complex (k_{-4}) would need to be substantially greater than k_{-2}. So, as with binding of non-cognate immunity proteins to the E9 DNase (Wallis et al., 1995a), the different binding affinities of Im9 for the different forms of the E9 DNase are influenced by the dissociation rate constants for the complexes.

Im8 binds to the E9 DNase but with a considerably faster rate of dissociation than for Im9: values of $k_{dissociation}$ measured by subunit exchange experiments are $28.2\ s^{-1}$ for Im8 (Wallis et al., 1995a) compared with $2.2 \times 10^{-6}\ s^{-1}$ for Im9 (Wallis et al., 1995b). Wallis et al. (1995a) showed that the Im8 interaction with the E9 DNase followed a similar kinetic scheme to that for Im9, but they also presented compelling evidence for at least three forms of the DNase being

present in equimolar solutions of E9 DNase and Im8 at equilibrium. Using Scheme 3, we would now say they are the N_A, N_B and N_BI forms. However, there must also be unbound Im8, and thus, unless K_4 is infinitesimally small, some of the N_AI form.

Stopped-flow fluorescence measurements of Im9 binding to the intact 61 kDa ColE9 show a similar biphasic time dependence to that for Im9 binding to the E9 DNase domain (Wallis et al., 1995b). Based on the above analysis, a similar slow conformational interchange of the DNase domain within the intact ColE9 must occur with similar kinetic and thermodynamic parameters to those of the E9 DNase (Table 3). Whether this assists the DNase domain in fulfilling its various roles by different conformational states having different functions, such as binding immunity protein tightly in the producing cell and hydrolysing DNA in the target cell, requires experimental investigation.

Acknowledgements

We gratefully acknowledge the Wellcome Trust for its award to G.R.M. of a Research Leave Fellowship, its funding of a 600 MHz NMR spectrometer at UEA and its general support of the UEA Colicin Research Group, and the EPSRC for its award of a studentship to S.B.-M.W. S.B.-M.W. also thanks Svenska Kulturfonden (Finland) for support. EPSRC and BBSRC are also acknowledged for their support of the UEA Colicin Research Group through their Biomolecular Sciences Panel, and for funding of the DMX500 spectrometer in the Biological NMR Centre at the University of Leicester. We thank Prof. D. Gani (St. Andrews) for helpful discussions concerning isomerisation of prolines.

References

Adjadj, E., Naudat, V., Quiniou, E., Wouters, D., Sautière, P. and Craescu, C.T. (1997) *Eur. J. Biochem.*, **246**, 218–227.

Bartels, C., Xia, T.-H., Billeter, M., Güntert, P. and Wüthrich, K. (1995) *J. Biolmol. NMR*, **5**, 1–10.

Cai, M., Zheng, R., Caffrey, M., Craigie, R., Clore, G.M. and Gronenborn, A.M. (1997) *Nat. Struct. Biol.*, **4**, 567–577.

Carlomagno, T., Mantile, G., Bazzo, R., Miele, L., Paolillo, L., Mukherjee, A.B. and Barbato, G. (1997) *J. Biomol. NMR*, **9**, 35–46.

Chak, K.-F., Kuo, W.-S., Lu, F.-M. and James, R. (1991) *J. Gen. Microbiol.*, **137**, 91–100.

Chazin, W.J., Kördel, J., Drakenberg, T., Thulin, E., Brodin, P., Grundström, T. and Forsén, S. (1989) *Proc. Natl. Acad. Sci. USA*, **86**, 2195–2198.

Cheng, H.N. and Bovey, F.A. (1977) *Biopolymers*, **16**, 1465–1472.

Creighton, T.E. (1993) *Proteins*, Freeman, New York, N.Y.

Curtis, M.D. and James, R. (1991) *Mol. Microbiol.*, **5**, 2727–2733.

Delaglio, F., Grzesiek, S., Vuister, G.W., Zhu, G., Pfeifer, J. and Bax, A. (1995) *J. Biomol. NMR*, **6**, 277–293.

Di Masi, D.R., White, D.C., Schnaitman, C.A. and Bradbeer, C. (1973) *J. Bacteriol.*, **115**, 506–513.

Eaton, T. and James, R. (1989) *Nucleic Acid Res.*, **17**, 1761–1761.

Ernst, R.R., Bodenhausen, G. and Wokaun, A. (1987). *Principles of NMR in One and Two Dimensions*, Clarendon Press, Oxford. Pp. 490–501.

Evans, P.E., Dobson, C.M., Kautz, R.A., Hartfull, G. and Fox, R.O. (1987) *Nature*, **329**, 266–268.

Falzone, C.J., Wright, P.E. and Benkovic, S.J. (1994) *Biochemistry*, **33**, 439–442.

Fejzo, J., Westler, W.M., Macura, S. and Markley, J.L. (1991) *J. Magn. Reson.*, **92**, 20–29.

Feng, Y., Klein, B.K., Vu, L., Aykent, S. and McWherter, C.A. (1995) *Biochemistry*, **34**, 6540–6551.

Feng, Y., Klein, B.K. and McWherter, C.A. (1996) *J. Mol. Biol.*, **259**, 524–541.

Garinot-Schneider, C., Pommer, A.J., Moore, G.R., Kleanthous, C. and James, R. (1996) *J. Mol. Biol.*, **260**, 731–742.

Grathwohl, C. and Wüthrich, K (1981) *Biopolymers*, **20**, 2623–2633.

Grzesiek, S. and Bax, A. (1992a) *J. Magn. Reson.*, **99**, 201–207.

Grzesiek, S. and Bax, A. (1992b) *J. Am. Chem. Soc.*, **114**, 6291–6293.

Grzesiek, S. and Bax, A. (1993) *J. Biomol. NMR*, **3**, 185–204.

Hinck, A.P., Loh, S.N., Wang, J. and Markley, J.L. (1990) *J. Am. Chem. Soc.*, **112**, 9031–9034.

James, R., Curtis, M.D., Wallis, R., Osborne, M.J., Kleanthous, C. and Moore, G.R. (1992). In Bacteriocins, Microcins and Lantibiotics (James, R., Lazdunski, C. and Pattus, F.), NATO ASI Series H, Springer, Heidelberg, pp. 181–201.

James, R., Kleanthous, C. and Moore, G.R. (1996) *Microbiology*, **142**, 1569–1580.

Jeener, J., Meier, B.H., Bachmann, P. and Ernst, R.R. (1979) *J. Chem. Phys.*, **71**, 4546–4553.

Kay, L.E., Keifer, P. and Saarinen, T. (1992) *J. Am. Chem. Soc.*, **114**, 10663–10665.

Kördel, J., Forsén, S., Drakenberg, T. and Chazin, W.J. (1990) *Biochemistry*, **29**, 4400–4409.

Li, W., Dennis, C., Moore, G.R., James, R. and Kleanthous, C. (1997) *J. Biol. Chem.*, **272**, 22253–22258.

Luria, S.E. and Suit, J.L. (1987) In Escherichia coli and Salmonella typhimurium, Cellular and Molecular Biology, Vol. 2 (Ed., Neidhardt, F.C.) Am. Soc. Microbiol., Washington, DC, pp. 1615–1624

Maia, H.L., Orrell, K.G. and Rydon, H.N. (1976) *J. Chem. Soc., Perkin Trans 2*, 761–763.

Marion, D., Driscoll, P.C., Kay, L.E., Wingfield, P.T., Bax, A., Gronenborn, A.M. and Clore, G.M. (1989a) *Biochemistry*, **28**, 6150–6156.

Marion, D., Ikura, M., Tschudin, R. and Bax, A. (1989b) *J. Magn. Reson.*, **85**, 393–399.

Ohno-Iwashita, Y. and Imahori, K. (1980) *Biochemistry*, **19**, 652–659.

Orrell, K.G., Sik, V. and Stephenson, D. (1990) *Prog. NMR Spectrosc.*, **22**, 141–208.

Osborne, M.J., Lian, L.-Y., Wallis, R., Reilly, A., James, R., Kleanthous, C. and Moore, G.R. (1994) *Biochemistry*, **33**, 12347–12355.

Osborne, M.J., Breeze, A.L., Lian, L-Y., Reilly, A., James, R., Kleanthous, C. and Moore, G.R. (1996) *Biochemistry*, **35**, 9505–9512.

Osborne, M.J., Wallis, R., Leung, K.-Y., Williams, G., Lian, L.-Y., James, R., Kleanthous, C. and Moore, G.R. (1997) *Biochem. J.*, **323**, 823–831.

Overduin, M., Tong, K.I., Kay, C.M. and Ikura, M. (1996) *J. Biomol. NMR*, **7**, 173–189.

Overmars, F.J.J. and Altona, C. (1997) *J. Mol. Biol.*, **273**, 519–524.

Palmer, III, A.G., Cavanagh, J., Wright, P.E. and Rance, M. (1991) *J. Magn. Reson.*, **93**, 151–170.

Palmer, III, A.G. (1997) *Curr. Opin. Struct. Biol.*, **7**, 732–737.

Pommer, A.J., Wallis, R., Moore, G.R., James, R. and Kleanthous, C. (1998) *Biochem. J.*, submitted.

Schaller, K. and Nomura, M. (1976) *Proc. Natl. Acad. Sci. USA*, **73**, 3989–3993.

Schmid, F.X. and Baldwin, R.L. (1978) *Proc. Natl. Acad. Sci. USA*, **75**, 4764–4768.

States, D.J., Haberkorn, R.A. and Ruben, D.J. (1982) *J. Magn. Reson.*, **48**, 286–292.

Steinberg, I.Z., Harrington, W.F., Berger, A., Sela, M. and Katchalski, E. (1960) *J. Am. Chem. Soc.*, **82**, 5263–5279.

Thomas, W.A. and Williams, M.K. (1972) *J. Chem. Soc., Chem. Commun.*, 994.

Toba, M., Masaki, H. and Ohta, T. (1988) *J. Bacteriol.*, **170**, 3237–3242.

Truckses, D.M., Somoza, J.R., Prehoda, K.E., Miller, S.C. and Markley, J.L. (1996) *Protein Sci.*, **5**, 1907–1916.

Wallis, R., Moore, G.R., Kleanthous, C. and James, R. (1992a) *Eur. J. Biochem.*, **210**, 923–930.

Wallis, R., Reilly, A., Rowe, A., Moore, G. R., James, R. and Kleanthous, C. (1992b) *Eur. J. Biochem.*, **207**, 687–695.

Wallis, R., Reilly, A., Barnes, K., Abell, C., Campbell, D.G., Moore, G.R., James, R. and Kleanthous, C. (1994) *Eur. J. Biochem.*, **220**, 447–454.

Wallis, R., Leung, K.-Y., Pommer, A.J., Videler, H., Moore, G.R., James, R. and Kleanthous, C. (1995a). *Biochemistry*, **34**, 13751–13759.

Wallis, R., Moore, G.R., James, R. and Kleanthous, C. (1995b) *Biochemistry*, **34**, 13743–13750.

Wallis, R., Leung, K.-Y., Osborne, M.J., James, R., Moore, G.R. and Kleanthous, C. (1998) *Biochemistry*, in press.

Willem, R. (1987) *Prog. NMR Spectrosc.*, **20**, 1–94.

Wüthrich, K. (1986) *NMR of Proteins and Nucleic Acids*, Wiley, New York, N.Y.

Zhang, O.W., Kay, L.E., Olivier, J.P. and Forman-Kay, J.D. (1994) *J. Biomol. NMR*, **4**, 845–858.

Zhu, G. and Bax, A. (1990) *J. Magn. Reson.*, **90**, 405–410.

Zuiderweg, E.R.P. and Fesik, S. (1989) *Biochemistry*, **28**, 2387–2391.